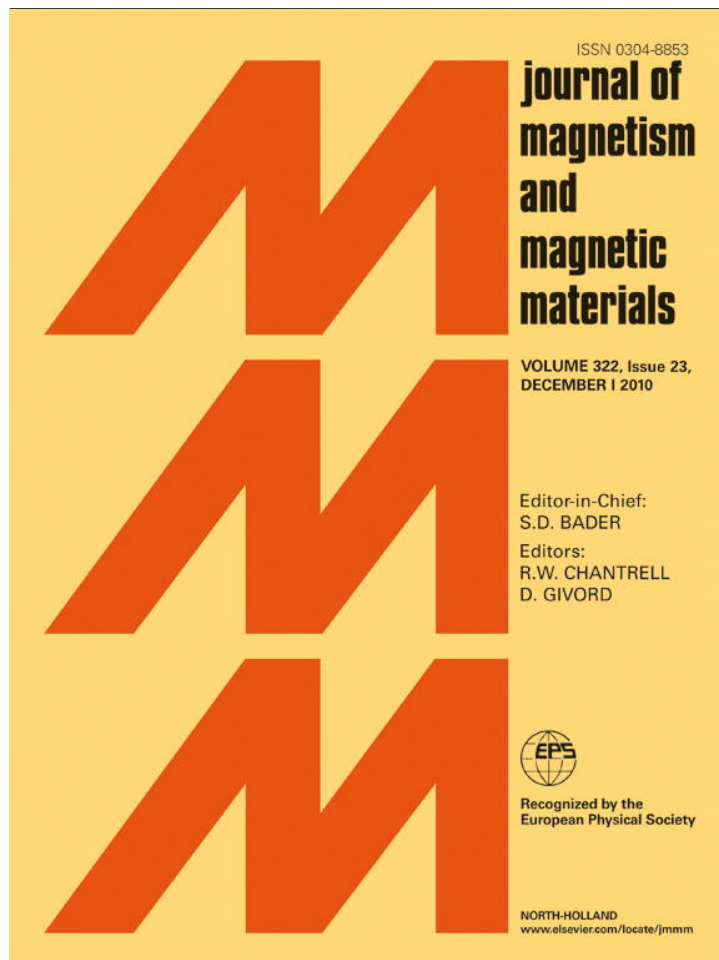


Provided for non-commercial research and education use.
Not for reproduction, distribution or commercial use.



This article appeared in a journal published by Elsevier. The attached copy is furnished to the author for internal non-commercial research and education use, including for instruction at the authors institution and sharing with colleagues.

Other uses, including reproduction and distribution, or selling or licensing copies, or posting to personal, institutional or third party websites are prohibited.

In most cases authors are permitted to post their version of the article (e.g. in Word or Tex form) to their personal website or institutional repository. Authors requiring further information regarding Elsevier's archiving and manuscript policies are encouraged to visit:

<http://www.elsevier.com/copyright>



Contents lists available at ScienceDirect

Journal of Magnetism and Magnetic Materials

journal homepage: www.elsevier.com/locate/jmmm

A Gaussian distribution model of anisotropic magnetorheological elastomers

W. Zhang, X.L. Gong*, L. Chen

CAS Key Laboratory of Mechanical Behavior and Design of Materials, Department of Modern Mechanics, University of Science and Technology of China, Hefei 230027, China

ARTICLE INFO

Article history:

Received 8 January 2010

Received in revised form

23 July 2010

Available online 7 August 2010

Keywords:

Gaussian distribution

Anisotropic

Magnetorheological elastomers

ABSTRACT

A Gaussian distribution model was developed to examine the field-induced performance of anisotropic magnetorheological elastomers. The developed model was based on the assumption that the iron particles in magnetorheological elastomers aggregate into a large number of parallel body-centered tetragonal structure columns whose length obeys the Gaussian distribution. By using multi-pole approximation with local field effect and taking into account the nonlinearity and saturation of particle magnetization, the field-induced shear modulus was calculated as a function of distribution and dimension of the particle structures, the external magnetic field and the dynamic shear strain. Compared with other modes as well as the published experimental results, this model shows a remarkable improvement in accurately predicting the behavior of the magnetorheological elastomers.

© 2010 Elsevier B.V. All rights reserved.

1. Introduction

Magnetorheological (MR) materials are a class of smart materials whose mechanical and magnetic properties can be varied by application of an external magnetic field [1]. Typically, they consist of micron sized magnetically permeable particles dispersed in a non-magnetic medium. Upon application of a magnetic field, these particles can form ordered structures that result in field-induced performance.

So far, many methods have been proposed to examine the field-induced behavior of MR materials. Bossis et al. [2] developed both the microscopic and macroscopic structural models to calculate yield stresses of MR fluids. Rosensweig [3] derived general expressions of the yield stress of the MR substance by taking into account unsymmetric elastic and magnetic stress states of a continuum. Ginder and Davis [4] analyzed average magnetic induction with the finite element analysis and computed the shear stresses from the field using Maxwell's stress tensor. Koon et al. [5] carried out research on Giant effect of magnetostriction materials. Guan et al. [6] presented results of the studies on magnetostrictive effect of the MRE. These methods are all based on the condition that the particles are dispersed in a fluid matrix. In this situation, the particles are subjected to small resistance and can form ordered column structures between two poles. However, the condition for MR elastomers is different as particles are hard to move freely in the elastomer matrix. Our microstructural observation also demonstrated that the particles could not form well-ordered column structures but can only form the discontinuous and finite

length structures [7]. Compared with electrorheological (ER) fluid and MR fluid research, very limited reports can be found, in the literature, to investigate the mechanism of MR elastomers. Jolly et al. [8] extended a simple dipole model, based on the magnetic interactions between two adjacent particles, to approximate MR elastomer performances. Davis [9] calculated the saturated field-induced shear modulus by considering the interactions in a single particle chain. It is noted that their models were based on the condition that particles within matrix can form well-ordered chain structures, which were not in good agreement with practical microstructural observations. For this reason, the present work aims to develop a model, by taking into account the practical microstructure, for accurately predicting the behavior of anisotropic MR elastomers. In the proposed model, a number of influencing factors, including the distribution and dimension of the particle columns, the nonlinear effect of external field, and shear strain, will be addressed.

2. The Gaussian distribution model approach

For ER and MR fluids, both theoretical [10] and experimental [11] studies proved that the body-centered tetragonal (BCT) structures were the mostly stable field-induced structures. Our microstructural study [7] also observed similar structures in MR elastomers. To this end, the proposed modeling approach is based on the assumption that the iron particles that have an average diameter of 2.5 μm in a matrix aggregate into a large number of BCT structures, which have the same direction, the same width but different length, as shown in Fig. 1(a), and this simplifies the calculations by assuming the chains are all neat and straight. And the BCT lattice can be regarded as a compound of chain of class A

* Corresponding author.

E-mail address: gongxl@ustc.edu.cn (X.L. Gong).

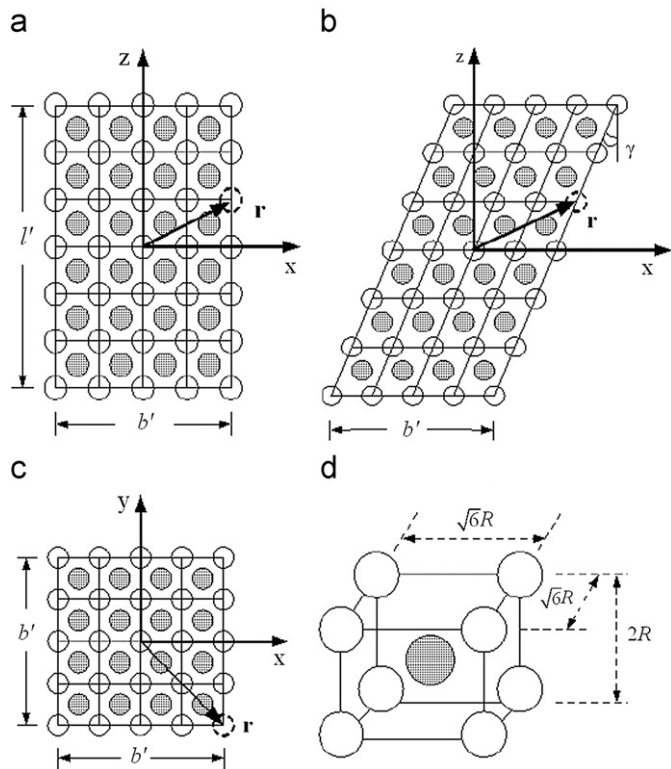


Fig. 1. A BCT column is viewed in the direction parallel to the z-axis when the MR elastomers (a) without external displacement, (b) under a shear strain γ , (c) the cross-section perpendicular to z-axis and (d) the dimension of each BCT cell [8]. The particles have radius R and are not shown to scale.

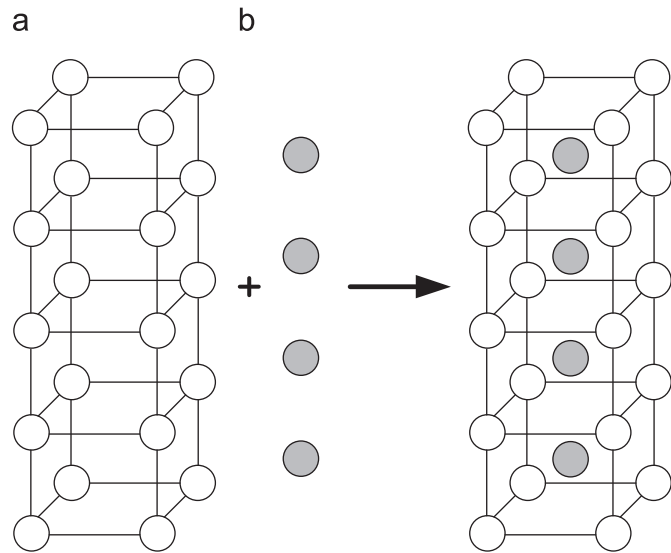


Fig. 2. The BCT lattice can be regarded as compound of chain of classes A and B. The empty and shadowed circles are denoted as the particles in chain of classes A and B, respectively.

and B, as shown in Fig. 2. We also assume that column length l' obeys the Gaussian distribution. Thus the numbers of particles l ($l=l'/2R+1 \geq 1$), along with each column, also obey the Gaussian distribution where the mean and the variance are represented by L and σ^2 , respectively. Due to the symmetry of the Gaussian distribution, the length l is assigned less than $2L$, i.e., $l \leq 2L$. Thus the value of l is distributed on the range of $[1, 2L]$. When the width of the column is b' , the number of particles in the width border is denoted by b where $b=b'/\sqrt{6}R+1$.

When an external magnetic field H_0 (in z-axis direction) is applied and a shear strain γ is imposed on the MR elastomers (Fig. 1b), their magnetic susceptibility is changed that leads to a magnetic field-induced shear stress τ , which can be expressed as [2]

$$\tau = -\frac{1}{2}\mu_0 \left(\frac{H_0}{1+\chi_{eff}} \right)^2 \frac{\partial \chi_{eff}}{\partial \gamma}, \quad (1)$$

where χ_{eff} is the effective magnetic susceptibility in the direction of the applied field, which is defined as

$$\chi_{eff} = \frac{J}{\mu_0 H_0}, \quad (2)$$

where J is the average particle polarization in the direction of the applied field in the MR elastomers. So J can be expressed as

$$J = \frac{\sum_{l=1}^{2L} (p_l n_l)}{V}, \quad (3)$$

where p_l and n , respectively, denote the total dipole moment in the z-axis direction and number of the columns that have number of l particles in the z-axis direction, and V is the volume of the whole MR elastomers.

Since the length of the columns obeys the Gaussian distribution, by using a constant factor k , n_l can be expressed as

$$n_l = k \frac{1}{\sqrt{2\pi}\sigma} e^{-(l-L)^2/2\sigma^2}. \quad (4)$$

The total number of particles in the z-axis direction in the whole MR elastomers can be obtained by the sum of that in all the columns:

$$N = \sum_{l=1}^{2L} (l n_l). \quad (5)$$

It can be seen from Fig. 1(c) that the number of particles in the cross-section of a column is $b^2 + (b-1)^2$. So N can also be calculated by

$$N = \frac{V\varphi}{V_p(b^2 + (b-1)^2)}, \quad (6)$$

where φ is the volume percentage of the particles, and V_p is the volume of each particle. From Eqs. (4)–(6), k can be obtained and n_l is given by

$$n_l = \frac{\varphi V e^{-(l-L)^2/2\sigma^2}}{V_p(b^2 + (b-1)^2) \sum_{l=1}^{2L} (l e^{-(l-L)^2/2\sigma^2})}. \quad (7)$$

Under the external magnetic field, a dipole moment is induced on each sphere particle. And the dipole moment will produce an additional magnetic field on the other dipole moments. So the dipole moment is affected by both the external magnetic field and other dipole moments. As the particles compose the BCT structures periodically, and for the sake of simplicity each particle in a column is assumed to have the same dipole moment.

p_l in Eq. (3) can be expressed by the sum of all the dipole moments in the columns, which have the number of l particles in the z-axis direction:

$$p_l = \sum^l p_{i,z} = n_l^l p_{i,z}, \quad (8)$$

where $p_{i,z}$ is the component in the z-axis direction of the dipole moment, and n_l^l , which is the number of particles in the columns that have number of l particles in the z-axis direction, is equal to $b^2 l + (b-1)^2 (l-1)$. In the following, $p_{i,z}$ is calculated by using a dipole approximation with local field effects.

\mathbf{H}_{loc} is the local field, which is the sum of the external field \mathbf{H}_0 and the field \mathbf{H}_p from all other dipoles evaluated at the position of the center of particle under consideration:

$$\mathbf{H}_{loc} = \mathbf{H}_0 + \mathbf{H}_p, \quad (9)$$

where

$$\mathbf{H}_p = \sum \frac{1}{4\pi\mu_0 r^5} (-r^2 \mathbf{p} + 3(\mathbf{p}\mathbf{r})\mathbf{r}), \quad (10)$$

where \mathbf{r} is the position vector relative to the origin and is summed over all other particles in the column under consideration. By setting the position of center particle in the column as the origin (as shown in Fig. 1(a)–(c)), the component of Eq. (10) in the z -axis is

$$H_{p,z} = \sum \frac{1}{4\pi\mu_0(x^2 + y^2 + z^2)^{5/2}} (-(x^2 + y^2 + z^2)p_z + 3z(p_x x + p_y y + p_z z)). \quad (11)$$

As the external field is in the direction of the z -axis, the dipole moment's components in x -axis and y -axis are ignored. Then Eq. (11) is simplified as

$$H_{p,z} = \sum \frac{2z^2 - x^2 - y^2}{4\pi\mu_0(x^2 + y^2 + z^2)^{5/2}} p_z. \quad (12)$$

$H_{p,z}$ is induced by the dipole moments in two class chains, A and B.

Firstly, the effect of class A chains is discussed. The particle's coordinate (x, y, z) is determined by two parts, which are the particle's relative position to the origin (A_1, A_2, A_3) and the shear strain γ . In Fig. 1(a) and (c), compared to the origin, the particle represented by the broken circle is the second particle in the x -axis direction, the second one in the y -axis negative direction, and the first one in the z -axis direction. So its relative position to the origin can be expressed as $(2, -2, 1)$, which is not changed by the shear strain. For class A chains, there is

$$\begin{aligned} x &= \sqrt{6}A_1R + 2A_3R\sin\gamma, \\ y &= \sqrt{6}A_2R, \\ z &= 2A_3R\cos\gamma. \end{aligned} \quad (13)$$

Substituting Eqs. (13) into (12), the range of the sum for integer A_1, A_2, A_3 is, respectively, $[-(b-1)/2, (b-1)/2]$, $[-(b-1)/2, (b-1)/2]$, $[-(l-1)/2, (l-1)/2]$ when b and l are odd numbers and $[-(b/2-1), (b/2-1)]$, $[-(b/2-1), (b/2-1)]$, $[-(l/2-1), (l/2-1)]$ when b and l are even numbers.

Similarly, for class B chains, there is

$$\begin{aligned} x &= \frac{\sqrt{6}}{2}(2B_1-1)R + 2(B_3-1)R\sin\gamma, \\ y &= \frac{\sqrt{6}}{2}(2B_2-1)R, \\ z &= 2(B_3-1)R\cos\gamma. \end{aligned} \quad (14)$$

Substituting Eqs. (14) into (12), the range of the sum for integer B_1, B_2, B_3 is respectively $[-(b-1)/2, 0]$ & $(0, (b-1)/2]$, $[-(b-1)/2, 0]$ & $(0, (b-1)/2]$, $[-(l-1)/2, 0]$ & $(0, (l-1)/2]$ when b and l are odd numbers and $[-b/2, 0]$ & $(0, b/2]$, $[-b/2, 0]$ & $(0, b/2]$, $[-l/2, 0]$ & $(0, l/2]$ when b and l are even numbers.

It is difficult to obtain the analytical expression for the relationship between $H_{p,z}$ and p_z from Eqs. (12)–(14) directly. Instead, we firstly set given values to b and γ , and a series of values to l , i.e. letting l be from 1 to 200. Then a series of values of $\Sigma(2z^2 - x^2 - y^2)/(4\pi\mu_0(x^2 + y^2 + z^2)^{5/2})$ (denoted by $\Sigma g(x, y, z)$ later) can be computed. By using high order (> 10) polynomial fitting, the expression $f(l)$ as a function of l is yielded, which can accurately predict each value of $\Sigma g(x, y, z)$. If the columns have different values of width or shear strain, the sum is recalculated

and a new $f(l)$ can be yielded. Here, the relationship is briefly given by

$$H_{p,z} = f(l, b, \gamma)p_z. \quad (15)$$

Under a low external magnetic field, a dipole moment induced linearly on each sphere particle is given by

$$p = 3\mu_e\mu_0\beta V_p H, \quad (16)$$

where μ_p and μ_e denote the relative permeability of the particles and elastomer matrix, respectively, and $\beta = (\mu_p - \mu_e)/(\mu_p + 2\mu_e) \approx 1$ when $\mu_p = 10^3$ and $\mu_e = 1$. At a high magnetic field, the magnetic nonlinearity and saturation of the particle magnetization are described by the Frohlich–Kennely law [10]:

$$M = \frac{p}{\mu_0 V_p} = \frac{\chi_l H}{1 + \chi_l H/M_s}, \quad (17)$$

where χ_l is the magnetic susceptibility in the low external field and M_s is the saturation magnetization. When the field is low, $\chi_l H/M_s$ is inclined to zero, and then Eq. (17) can be degraded into

$$p = \mu_0 V_p \chi_l H. \quad (18)$$

By comparing Eqs. (16) and (18), χ_l is obtained. Substituting into Eq. (17), the relation between the dipole moment and the magnetic field can be rewritten as

$$p = \frac{3\mu_e\mu_0\beta V_p H}{1 + 3\mu_e\beta H/M_s}. \quad (19)$$

From Eqs. (9), (15) and (19), p_z is obtained as a function of external field (H_0), particle numbers in the column's length and width direction (l and b), and the imposed shear strain (γ). Combining this result with Eqs. (2), (3), (7) and (8), the effective magnetic susceptibility χ_{eff} is obtained. On the other hand,

$$\begin{aligned} \frac{\partial \chi_{eff}}{\partial \gamma} &= \frac{\partial \chi_{eff}}{\partial f(l, b, \gamma)} \frac{\partial f(l, b, \gamma)}{\partial \gamma} \\ &= \frac{\partial \chi_{eff}}{\partial f(l, b, \gamma)} \frac{\partial \Sigma g(x, y, z)}{\partial \gamma} \\ &= \frac{\partial \chi_{eff}}{\partial f(l, b, \gamma)} \Sigma \frac{\partial g(x, y, z)}{\partial \gamma} \\ &= \frac{\partial \chi_{eff}}{\partial f(l, b, \gamma)} k(l, b, \gamma), \end{aligned} \quad (20)$$

where $k(l, b, \gamma)$ is the polynomial fitting result of the $\Sigma(\partial g(x, y, z)/\partial \gamma)$. By substituting the results of χ_{eff} and $\partial \chi_{eff}/\partial \gamma$ into Eq. (1), the field-induced shear strain is solved and the field-induced shear modulus (ΔG) is calculated accordingly. In order to compare with previous experimental results [7], in the present calculation, the iron particle volume percentage is set as 11% and the shear strain is set as 0.003 (except for research on the effect of shear strain, shown in Fig. 6).

3. Results and discussions

Our previous experimental results [12] indicated that the shear modulus of MR elastomers was typically saturated before the external magnetic field reaching 1 MA/m. In this simulation, the magnetic saturation field strength is set as $H_0 = 1$ MA/m. Under this magnetic field, the MR elastomers' saturated field-induced shear modulus, for various particle columns with different mean and variance of the length of particle columns, was calculated and shown in Fig. 3. It is seen that the modulus increases with the value of L and then gradually rises to a maximum. The smaller the variance, the more quickly the field-induced modulus reaches the maximum. This result implies that

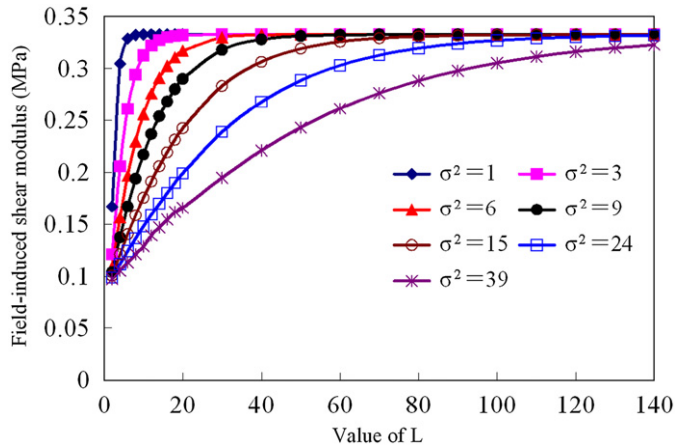


Fig. 3. The field-induced shear modulus of MR elastomers when the value of mean and the variance of length of columns are varied. Here, MR elastomers are assumed to be exposed in a high magnetic field (1 MA/m), and with the same width of the columns ($b=2$).

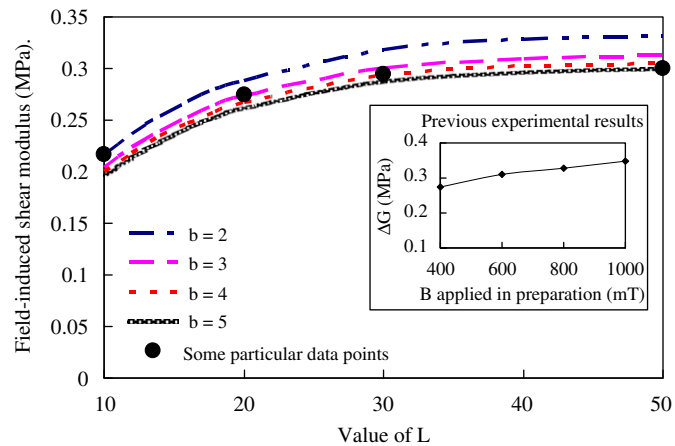


Fig. 4. The calculated field-induced shear modulus of MR elastomers with different width columns. In calculation, the external field H_0 is set as 1 MA/ and the variance is set as 9. Inset: the previous experimental results of field-induced shear modulus of MR elastomers prepared in different magnetic flux densities [5].

the fabrication of MR elastomers with long columns is greatly helpful to obtain the high effect. This can be achieved by applying the strong field in curing time, using the low viscosity matrix and adding high percentage iron particles. The result also suggests that it is important to concentrate the length of column in the mean value instead of the distribution in a wide range, as the shear modulus of columns at a small mean length could still rise to a large value if the variance is small. Therefore, curing time should be prolonged, so that the particles have enough time to aggregate into the columns with the same length in the external uniform magnetic field.

In the microstructures and dynamic properties observed previously [9], the saturated shear modulus was enhanced as the increase of length of the short column (about less than 30 particles in the length direction), and it has little change as the increase of length of the long column (about more than 80 particles in the length direction).

At a constant variance of 9, the field-induced modulus versus the particle column width is calculated and shown in Fig. 4. As can be seen from this figure, the shear modulus has an initially evident decrease when the value of b is raised from 2 to 3; then it shows a slightly decreasing trend when the value of b is further

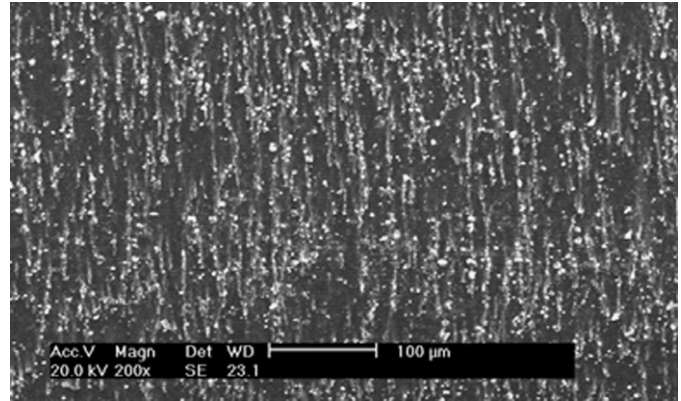


Fig. 5. Microscopic observations of MR elastomers samples by SEM.

increased. The previous observation [7] shows that the length and the width of the columns were both increased by the increment of the magnetic flux density applied in preparation. For the MR elastomers prepared in magnetic flux densities of 400, 600, 800 and 1000 mT, the interparticles aggregated into column structures, which were consistent with the proposed model. The mean particle numbers in length and width direction were measured as $(L=10, b=2)$, $(L=20, b=3)$, $(L=30, b=4)$ and $(L=40, b=5)$ roughly. And the microscopic observations of MR elastomers samples are also shown in Fig. 5. It can be observed that the chains have different lengths and widths, which can qualitatively support the calculation results that the mean particle numbers in length and width directions obey the Gaussian distribution. The calculated field-induced shear moduli at these points were marked with black dots in Fig. 4, and the experimental saturated field-induced shear modulus of MR elastomers prepared in different magnetic flux density was inserted in Fig. 4. It is illustrated in Fig. 4 that the calculated and experimental results agreed with each other within allowed errors. The small discrepancy between them may be due to the ignorance of the interaction among the particle columns. Indeed, the proposed model improves the accuracy by multi-pole approximation where the interaction among all the particles in the column is considered.

The results of saturated field-induced shear modulus of other MR elastomers models, which are based on the magnetic interactions between two adjacent particles [7] and among the particles in a single chain [8], are, respectively, 0.11 and 0.19 MPa, which are both lower than the results of experimental and our Gaussian distribution model.

The effect of external magnetic field strength and shear strain amplitude on the field-induced shear modulus is illustrated in Fig. 6. At any of applied shear strains from 0.001 up to 0.005, the shear modulus increases steadily as the magnetic field increases. The increasing trend shows a decreasing trend with magnetic field, which is due to the nonlinearity and saturation of the particle magnetization and is able to well explain the previous experimental evidences. On the other hand, it can be seen from Fig. 6 that field-induced shear modulus also has great dependence on the amplitude of shear strain. At an external field of 1 MA/m, the shear modulus of MR elastomers at the shear strain of 0.005 is 0.19 MPa. It can sharply rise to 0.99 MPa when the shear strain reduces to 0.001. Fig. 6 indicates that the field-induced shear modulus is nearly inversely proportional to the shear strain. Similar results were reported by experimental studies [12,13]. The present result might be helpful to the dynamic application designed based on MR elastomers. In order to obtain a high MR effect, their dynamic strain should be controlled in a low level.

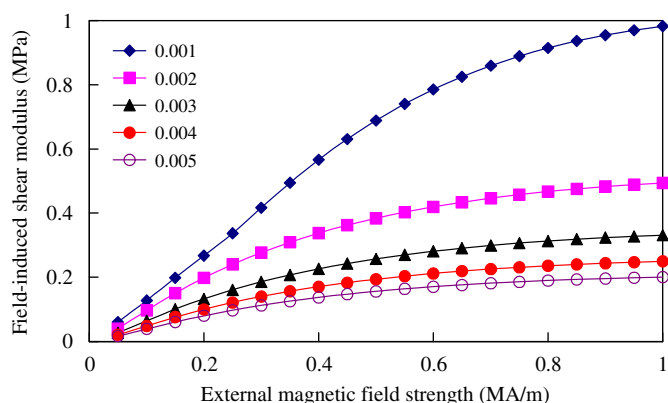


Fig. 6. The field-induced shear modulus of MR elastomer under different magnetic fields and stress shear strains.

Furthermore, it is interesting to notice in Fig. 6 that the MR elastomers under the small strain cannot be saturated until a strong field is applied. When the amplitude of strain is 0.001, the shear modulus does not reach a maximum even though the external field is at 1 MA/m.

4. Conclusions

A Gaussian distribution model that examines the field-induced shear modulus of the anisotropic MR elastomers has been presented. The calculation results show that the field-induced shear modulus was greatly affected by the distribution of the length of the particle columns. High modulus can be induced when the mean value of the length is large and the length is concentrated in the mean value instead of distributed in a wide range. The width of the columns also shows a slight influence on

the field-induced modulus. The thin columns can result in a little better MR effect than the thick ones. In addition, it is also demonstrated that the external field strength and shear strain both have a nonlinear impact on the behavior of MR elastomers.

The calculation result of the Gaussian distribution model is also compared with other conventional models and the relevant published data. It is shown that this model agrees well with the experimental evidence and indeed improves the accuracy of prediction behavior of the magnetorheological elastomers.

Ongoing work on modeling of MR elastomers behaviors will consider the magnetic interaction among the particle columns and take the magnetic flux density distribution within the particle network into account.

Acknowledgements

Financial support from SRFDP of China (Project no. 20093402110010) is gratefully acknowledged.

References

- [1] J.D. Carlson, M.R. Jolly, *Mechatronics* 10 (2000) 555.
- [2] G. Bossis, E. Lemaire, O. Volkova, *J. Rheol.* 41 (1997) 687.
- [3] R.E. Rosensweig, *J. Rheol.* 39 (1995) 179.
- [4] J.M. Ginder, L.C. Davis, *Appl. Phys. Lett.* 65 (1994) 3410.
- [5] N.C. Koon, C.M. Williams, B.N. Das, *J. Magn. Magn. Mater.* 100 (1991) 173.
- [6] X.C. Guan, X.F. Dong, J.P. Ou, *J. Magn. Magn. Mater.* 320 (2008) 158.
- [7] L. Chen, X.L. Gong, W.H. Li, *Smart Mater. Struct.* 16 (2007) 2645.
- [8] M.R. Jolly, J.D. Carlson, B.C. Munoz, *Smart Mater. Struct.* 5 (1996) 607.
- [9] L.C. Davis, *J. Appl. Phys.* 72 (1992) 1334.
- [10] R. Tao, J.M. Sun, *Phys. Rev. Lett.* 67 (1991) 398.
- [11] L. Zhou, W. Wen, P. Sheng, *Phys. Rev. Lett.* 81 (1998) 1509.
- [12] L. Chen, X.L. Gong, W.Q. Jiang, J.J. Yao, H.X. Deng, W.H. Li, *J. Mater. Sci.* 42 (2007) 5483.
- [13] C. Bellan, G. Bossis, *Int. J. Mod. Phys. B* 16 (2002) 2447.